Journal of Photochemistry and Photobiology A: Chemistry 302 (2015) 69–77

Contents lists available at ScienceDirect

Journal of Photochemistry and Photobiology A: Chemistry

journal homepage: www.elsevier.com/locate/jphotochem

Photoprocesses of alkyl *meso*-thiacarbocyanine dyes in the presence of cucurbit[7]uril

Galina V. Zakharova [a], Dmitrii A. Zhizhimov [a], Sergey K. Sazonov [a], Vitaly G. Avakyan [a], Sergey P. Gromov [a], Helmut Görner [b], Alexander K. Chibisov [a,*]

[a] Photochemistry Center, Russian Academy of Sciences, Moscow 119421, Russian Federation
[b] Max-Planck-Institute for Chemical Energy Conversion, D-45413 Mülheim an der Ruhr, Germany

ARTICLE INFO

Article history:
Received 13 November 2014
Received in revised form 22 January 2015
Accepted 24 January 2015
Available online 28 January 2015

Keywords:
Cyanine dyes
Cucurbiturils
Monomeric inclusion complexes
Dimeric inclusion complexes
Absorption
Delayed fluorescence
Quantum chemical calculations

ABSTRACT

The effects of cucurbit[7]uril, CB7, on the photophysical processes of 3,3′-diethyl-9-methylthiacarbocyanine iodide (**1**), 3,3′-dihydroxyethyl-9-methylthiacarbocyanine chloride (**2**) and 3,3′-diethyl-5,5′-dichloro-9-ethylthiacarbocyanine *p*-toluene sulfonate (**3**) were studied in phosphate buffer (pH 6.86) mostly at room temperature. Dyes **1**–**3** are cationic and present as equilibrated mixtures of monomers and dimers. Without CB7 the monomers demonstrate low yield of fluorescence which is increased 7–15 fold in the presence of CB7 as a result of formation of monomeric inclusion complexes. The dimers practically do not fluoresce. In the presence of CB7 the dimers produce dimeric inclusion complexes which exhibit both prompt and delayed fluorescence. The portion of delayed fluorescence is 0.08–0.1 of the total emission and the lifetimes are 0.07, 0.1, 0.25 ms for **1**, **2** and **3** respectively. The presence of monovalent metal ions or ammonium cation in aqueous solution of the dyes is prerequisite for delayed fluorescence of dimeric inclusion complexes. On the basis of quantum-chemical calculations the proposed structure of dimeric inclusion complex is characterized by near parallel orientation of two π-stacking chromophores retaining planar configuration, whereby each of them is partly inserted into the CB7 inner cavity. The difference in counter ions (chloride and *p*-toluene sulfonate) is reflected in the structure of dimeric inclusion complexes.

1. Introduction

Cucurbit(n)urils, CB(n), $n = 6/8$, represent an attractive class of water-soluble macrocyclic cavitandes forming stable inclusion complexes with either neutral or, mostly, positively charged molecules by insertion of organic residues in CB(n) hydrophobic cavities [1–3]. CB(n) are important for many applications, such as drug delivery [4], molecular recognition [5,6] or supramolecular catalysis [7–9]. In the past decade much attention has been paid for the formation of CB(n) inclusion complexes with organic dyes [10–13]. Dye encapsulation in CB(n) macrocycle was suggested to improve the solubility, prevent undesirable aggregation and increase the photostability of many organic dyes [10,14]. The embedding of dyes in CB(n) cavities results in bathochromic or hypsochromic shifts of the absorption and fluorescence maxima [13,15–17] along with increasing the lifetime and quantum yield of fluorescence of the dyes [10,12,13,18,19].

Among various organic compounds the cyanines dyes (Cy) represent an important class of synthetic dyes [20,21]. Primarily the Cy were used as spectral sensitizers in conventional silver halide photography [22,23]. Recently, new applications of Cy were reported, in particular, J-aggregates in electroluminescence [24–26] as well as in non-linear optical devices [27]. Cy often serve as luminescent labels and their fluorescent properties depend on the dyes structure and their environment [28]. The formation of complexes between Cy and CB(n), Cy@CB(n), might expect to influence photophysical and photochemical properties of the dyes resulting in changes of fluorescent yield, intersystem crossing probability, lifetime of the excited singlet state, kinetics of *cis* → *trans* thermal isomerization and electron transfer.

It is known that monomeric Cy without alkyl substituent in the *meso*-position of the polymethine chain demonstrate the ability to efficient *trans* → *cis* photoisomerization in solution which proceeds via the excited singlet state [29]. For many Cy backward *cis* → *trans* thermal isomerization occurs in the μs–ms time scale. The formation of inclusion complexes between CB7 and Cy, in particular with 3,3′-diethylthiazolinocarbocyanine, results in an increase of the lifetime of the *cis*-isomer [30]. In the presence of

* Corresponding author. Tel.: +74959361204; fax: +74959361255.
E-mail address: alexander.chibisov@gmail.com (A.K. Chibisov).

http://dx.doi.org/10.1016/j.jphotochem.2015.01.011
1010-6030/

CB7 the rate of *cis* → *trans* thermal isomerization is decreased due to sterically hindered rotation around the C=C double bond of the polymethine chain. Thus complexation might be the tool to control the rate of *cis* → *trans* thermal isomerization.

Fluorescent intensity of monomer Cy is known to be substantially increased for Cy@CB(*n*) complexes. In particular, CB7 was found to exert a significant influence on the fluorescence of 3,3′-diethylthiazolinocarbocyanine [30], 3,3′-diethylthiacarbocyanine [19] and 3,3′-diethyl-5,5′-dichloro-9-ethylthiacarbocyanine [31], enhancing thereby, due to formation of the monomeric inclusion complexes, the fluorescence yield in aqueous solution by two, five and seven times, respectively. Besides the presence of CB7 results in an increasing of the lifetime of the excited singlet state of 3,3′-diethylthiacarbocyanine [19], 3,3′-disulfopropylindocarbocyanine and 3,3′-disulfopropylindodicarbocyanine [10].

It is known that free Cy and especially sulfoalkyl *meso*-ethylthiacarbocyanines demonstrate an ability to form dimers in aqueous solution [32,33]. Although the dimers of Cy as well as of many other dyes are usually nonfluorescent, the dimers of thiamonomethinecyanines and thiacarbocyanines were found to show a weak fluorescence [32,34].

The interaction of Cy with CB(*n*) might result in the formation of dimeric complexes which exhibit fluorescence. Recently it was found that 2:2 stoichiometric complexes of 1-methyl-4-[(3-methyl-2(3H)-benzothiazolylidene) methyl]quinolinium *p*-tosylate with CB(8) are actually dimeric inclusion complexes; they exhibit spectacular fluorescence enhancements of up to 1700 fold [35]. Such an extraordinary increase of fluorescence yield of complexes stimulates exploratory researches of new systems that might be perspective as luminescent chemosensors.

In our previous communication [31] it has been shown that 3,3′-diethyl-5,5′-dichloro-9-ethylthiacarbocyanine *p*-toluene sulfonate forms in the presence of both CB7 and metal cations a dimeric inclusion complex showing a delayed fluorescence. The later is in favour of population of the triplet state of the complexes. Earlier we have shown [36] that the dimers of sulfoalkyl *meso*-ethylthiacarbocyanine dyes in the triplet state react with *p*-nitroacetophenone as an electron acceptor yielding the corresponding dimeric anion radicals which appeared to be unstable and dissociate during 10 μs into the neutral dye radicals and monomeric dye anions. Similarly unstable dimeric radicals have been reported for rhodamine 6G dimers [37]. The dimeric inclusion complexes with CB7 are expected to react with electron donors or acceptors, and CB7 might play a role of stabilizer of dye radicals.

It is important to learn whether or not the dimeric complex of 3,3′-diethyl-5,5′-dichloro-9-ethylthiacarbocyanine *p*-toluene sulfonate formed with CB7 is exceptional, and the relative cyanine dyes are also able to form inclusion complexes which are characterized by delayed fluorescence.

In this paper we continued our research on photoprocesses of alkyl *meso*-thiacarbocyanine dyes (3,3′-diethyl-9-methylthiacarbocyanine iodide (**1**), 3,3′-dihydroxyethyl-9-methylthiacarbocyanine chloride (**2**) and 3,3′-diethyl-5,5′-dichloro-9-ethylthiacarbocyanine *p*-toluene sulfonate (**3**) in the presence of cucurbit(7)uril mostly at room temperature in phosphate buffer. The choice of these dyes was motivated by the following reasons. The dyes are cationic that facilitate the formation of inclusion complexes with CB7. The dyes are structurally similar but they are distinguished mostly by the presence of chlorine substituents at 5,5′ position in benzothiazole residue for **3** which is known to be essential for aggregation [23,33]. Besides the presence of alkyl substituent in the *meso*-position plays a key role in the formation of dimeric inclusion complexes [23]. Quantum-chemical calculations were used to shed light on the structure of the complexes and find out the energetic parameters of complexation.

2. Experimental

2.1. Materials

The cyanines **1**–**3** were the same as used previously [38,39]. Structure of dyes **1**–**3** are compiled in Table 1.

CB7 from Strem Chemicals was used as commercially available. Water was from a Millipore (Milli-Q) system; methanol and acetonitrile were from Merck and used as received. Measurements were carried out mostly at room temperature in phosphate buffer (KH_2PO_4, Na_2HPO_4, 12 mM, pH 6.86) unless otherwise indicated. Dissolved oxygen was removed from the solutions by bubbling with argon.

2.2. Methods

A diode spectrophotometer (Agilent 8453) was employed for steady-state absorption spectra measurements. A spectrofluorimeter (Cary, Eclipse) was operating both in "fluorescence" and "phosphorescence" modes. The specificity of the spectrofluorimeter consists in the presence of the flash lamp as the excitation source. The spectrofluorimeter was used to measure spectra of prompt and delayed fluorescence as well as the decay kinetics of delayed fluorescence. Those have been measured using a delay of 100 μs after the cease of flash lamp emission that completely excludes the interference from prompt fluorescence and pulsed stray light. The dye concentration varied in the range of 1–20 μM for absorption and 1–2 μM for fluorescence.

Table 1
Structure of dyes 1–3.

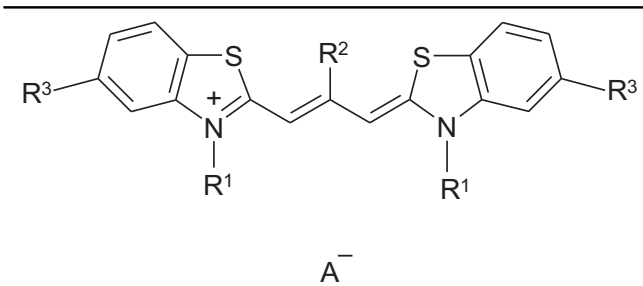

Dye	R^1	R^2	R^3	A
1	C_2H_5	CH_3	H	I
2	$(CH_2)_2OH$	CH_3	H	Cl
3	C_2H_5	C_2H_5	Cl	TsO

2.3. Quantum chemical calculations

The calculations were performed for **1**–**3** and their inclusion complexes. A semi-empirical method PM3 with the standard set of parameters was used to calculate structures of the dyes, their monomeric and a dimeric inclusion complexes with CB7 as well as the energy of complexation. Complete optimization of geometry parameters were performed using the suite of program FIREFLY: http://quantum-2.chem.msu.ru/gran/gamess/index.html HyperChem package 8.0 (Hypercube Inc.) was used to prepare the starting files and visualize the results. To determine a point group of symmetry for starting and resulting systems the ChemCraft program with version 1.7: www.chemcraftprogram.com was used. As usually, complex formation energies were estimated by subtraction of the sum of the component heats of formation from the total energy of the complex.

3. Results and discussion

3.1. Absorption

The absorption spectrum of **1**–**3** in organic solvents consists of one intense band in the visible with λ_{max} = 541 nm for **1** in acetonitrile. The absorption spectra of **2** and **3** are similar to that of **1** but they are distinguished by the position of the principal band for **2** (λ_{max} = 546 nm) and for **3** (λ_{max} = 552 nm) in acetonitrile [39,40]. In water a new blue shifted band of lower intensity appears at 502 nm for **1** and at 508 nm for **2** which looks like a shoulder (Fig. 1(a) and (b)). As regards **3** a new band is characterized by distinct maximum at 513 nm (Fig. 1(c)).

A new band for **3** and a shoulder for **1** and **2** disappear on addition to aqueous solution a certain amount of methanol or acetonitrile (not shown). This is assigned to dimers which dissociate into monomers. The dimers as the simplest aggregates with the parallel alignment of the transition moments (sandwich-type structure) are known to be characterized by absorption bands which are blue shifted with respect to those of monomers [32,33]. Upon increasing the dye concentration (i.e., 100-fold) a series of blue-shifted bands (H-bands) became apparent. Application of the exciton model then led to the identification of these H-bands as *n*-mers, i.e. trimers, tetramers and higher order aggregates [33]. In the present work we did not observe additional bands which should be assigned to higher order aggregates, i.e., H- and/or J-aggregates.

Increasing the dye concentration results in a shifting of the monomer (M) – dimer (D) equilibrium towards the free dimer. The insets of Fig. 1 display the increase of absorbance at 502 nm for **1**, 505 nm for **2** and 509 nm for **3** with increasing dyes concentration. However, it is quite reasonable that blue-shifted shoulders for **1** and **2** might be due to weak vibronic bands that overlap with the dimer band.

A similar behaviour, i.e., formation of dimers with increasing dye concentration, was found for other cyanine dyes [32]. From the comparison of the shape of absorption spectra it follows that spectra of **1** and **2** are similar in contrast to that of **3**. The blue shifted absorption band is characterized by a higher absorbance for **3** indicating a more efficient dimerization with respect to those of **1** and **2.** We suppose that the difference in the dimerization efficiency is due to a specific structure of **3** caused by chlorine as substituents at 5,5′ positions. The presence of chlorine atoms in the framework of thiacarbocyanine dyes is known to promote the formation of dimers and higher aggregates e.g., J-aggregates [23,33].

Absorption spectra of **1**–**3** in aqueous solutions were also measured on addition of CB7. The specificity of CB7 is that its presence in the solution results in a decrease of pH value down to 4.2 that gives rise to significant bleaching of the absorption bands. The absorbance was found to be recovered and kept constant when the measurements were either carried out in phosphate buffer (pH 6.86) or in aqueous solution in the presence of NH_4OH (pH 7). Thus spectral measurements with **1**–**3** in the presence of CB7 were made preferentially in phosphate buffer.

Fig. 1 also shows the absorption spectra of **1**–**3** in the presence of CB7. It is important to note that the presence of CB7 in aqueous solutions results in a bathochromic shift of the principal absorption band for all three dyes and its decrease for **1** and **2** in contrast to **3**. Since CB7 does not have any absorption in the visible region, we suggest that the shifting is in favour of the formation of monomeric inclusion complexes, **1**@CB7, **2**@CB7, **3**@CB7 between the monomers **1, 2, 3** and CB7, respectively. Regarding **3** the presence of CB7 in aqueous solutions gives rise to increasing of the principal absorption band and decreasing of the dimeric band at 509 nm. This effect is caused by a disaggregation of the dimers under the influence of CB7 that results in an increase of the concentration of dye monomers. The later leads to an additional amount of monomeric inclusion complexes. Besides, a new band appears at 514 nm for **1**, 510 nm for **2** and 528 nm for **3**. We suggest that this is the result of dimerization of monomeric inclusion complexes **1**@CB7, **2**@CB7 and **3**@CB7 giving rise to formation of the dimeric inclusion complexes $(\mathbf{1}@CB7)_2$ $(\mathbf{2}@CB7)_2$ and $(\mathbf{3}@CB7)_2$.

In order to establish the complex composition and to determine the association constant between the dyes and CB7, spectrophotometric titrations were made. The measurements of UV–vis absorbencies for (**1**–**3**)@CB7 were carried out as the function of CB7 concentration. The HypSpec software (Hyperquad) [41] was applied to determine the stoichiometry of complexes. However, there arouse a problem due to existence of a few equilibria, e.g., monomer-dimer for both free dyes and their complexes with CB7 that results in the lack of an isosbestic point in absorption spectra and prevents an evaluation of data by means of the Hyperquad software. We believe that the formation of the dimeric

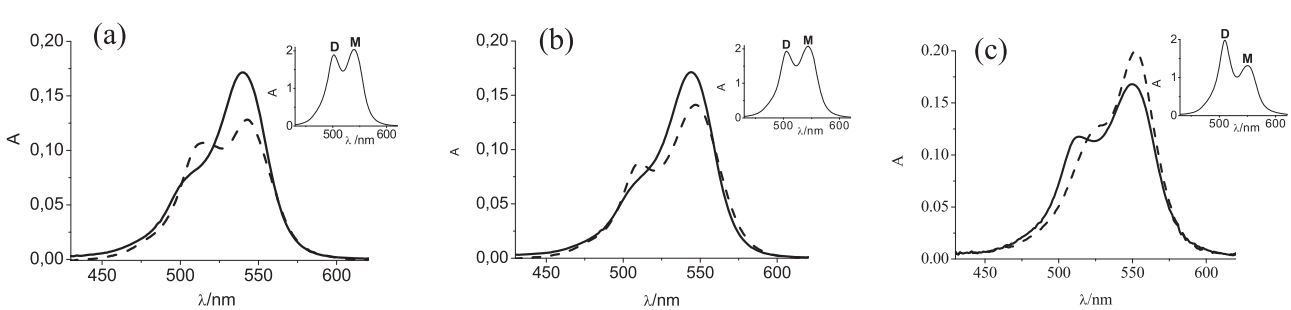

Fig. 1. Absorption spectra of **1**(a), **2**(b) and **3**(c) (1.5 μM) in the absence (solid) and in presence of CB7 (0.5 mM, dash) in phosphate buffer. Inset: absorption spectra of **1–3** (15 μM).

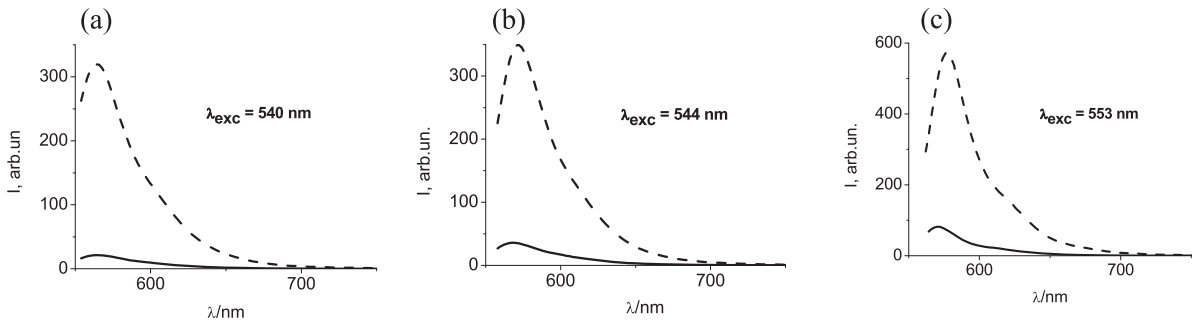

Fig. 2. Fluorescence spectra of **1**(a), **2**(b) and **3**(c) (1.5 μM) in the absence (solid) and in presence (dash) of 0.5 mM CB7 in phosphate buffer.

inclusion complex occurs as a result of dimerization of the primarily formed monomeric inclusion complex. For all three dyes the absorption band of the dimeric complex disappeares upon addition of a certain amount of acetonitrile (not shown) to the buffer solution. This is the result of their dissociation into monomeric dyes and CB7.

3.2. Fluorescence

Free monomers of **1**, **2** and **3** in buffer solution were found to exhibit low intensity fluorescence peaking at 565, 568 and 570 nm, respectively (Fig. 2) when the measurements were made in "fluorescence" mode. The fluorescence failed to detected when the measurements were made in "phosphorescence" mode. Thus low intensity fluorescence should be assigned to prompt fluorescence of the monomers.

Addition of CB7 to the dye in buffer solution results in a shifting of the fluorescence maximum to longer wavelengths by 1, 4 and 7 nm with respect to those of the free monomers **1**, **2** and **3**, respectively. This is due to formation of monomeric inclusion complexes. The intensity of fluorescence of monomeric inclusion complexes was found to be much higher than that for free monomers, namely, by 15 times for **1,** 10 times for **2** and 7 times for **3** in the presence of 0.5 mM CB7 (Fig. 2). These results together with absorption spectra (Fig. 1) reflect a behaviour which is specific for monomeric inclusion complexes.

Since *trans* → *cis* photoisomerization and fluorescence are competing processes the inhibition or a suppress of the photoisomerization should result in an increase of the fluorescence intensity. The former might be due to sterically hindered rotation of the benzothiazole residues around the C=C double bond of the polymethine chain. Thus one might expect that the complexation gives rise to a decrease of the quantum yield of *trans* → *cis* photoisomerization and an increase of that of fluorescence. The fluorescence enhancement in the presence of CB7 has also been established for certain other dyes [12,13,15–19,30].

Along with observation of fluorescence of the monomers and monomeric inclusion complexes the dimeric inclusion complexes were also found to demonstrate fluorescence. Since the absorption spectra of the monomeric and dimeric inclusion complexes overlap (Fig. 1) the excitation of dimeric inclusion complexes result partly in excitation of monomeric complexes. Figs. 3 and 4 display fluorescence spectra of inclusion complexes where the peaks at 565 (Fig. 3a), 570 nm (Fig. 3b) and 578 nm (Fig. 4) are assigned to fluorescence of monomeric inclusion complexes of **1**, **2** and **3**, respectively. Moreover, the bands peaking at 600 (Fig. 3a), 616 nm (Fig. 3b) and 622, 670 nm (Fig. 4) were assigned to fluorescence of the dimeric inclusion complexes (**1**@CB7)$_2$ (**2**@CB7)$_2$ and (**3**@CB7)$_2$, respectively. This is confirmed by an analysis of the fluorescence excitation spectra (not shown). Note that otherwise the term fluorescence refers to emission.

Since the obtained results appeared to be more pronounced for **3** a further analysis of experimental data was carried out mostly for dimeric inclusion complexes ((**3**@CB7)$_2$. The reason might be due to a specificity of the structure of **3** which is characterized by the presence of chlorine atoms in the framework of the dye.

With increasing of the CB7 concentration the yield of fluorescence of monomeric complex is approaching the saturation limit (inset in Fig. 4) in contrast to that for fluorescence of a dimeric inclusion complex. It was impossible to perform measurements at higher CB7 concentration due to its low solubility. The determination of the composition of the complexes and determination of the association constants by means of fluorescence titration failed due to overlapping of absorbencies of monomeric and dimeric inclusion complexes, thereby preventing any selective excitation. An intensive band at 628 nm and a two fold less intensive band at 674 nm were detected in the "phosphorescence" mode (Fig. 5c) and assigned to delayed fluorescence. The difference in wave numbers of two bands is 1087 cm^{-1} pointing to a weak vibronic transition at 674 nm. A delayed fluorescence was also observed for the dimeric inclusion complexes of **1** and **2.** The maxima of delayed fluorescence of these complexes are compiled in Table 2. A weak

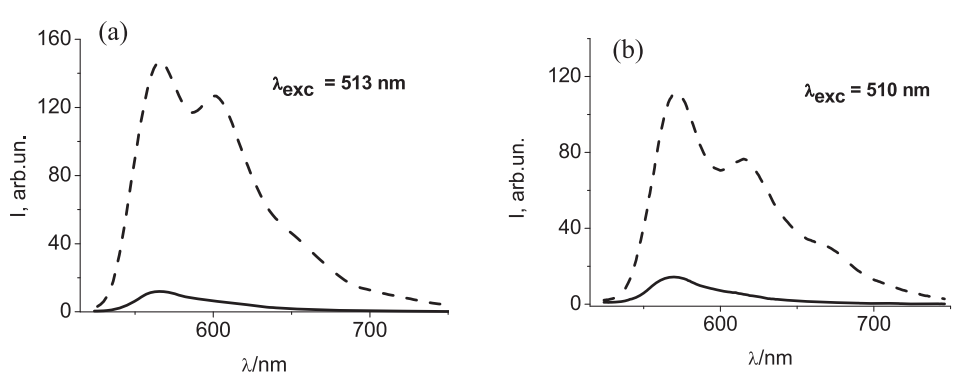

Fig. 3. Fluorescence spectra of **1**(a) and **2**(b) (1.5 μM) in the absence (solid) and in presence (dash) of 0.5 mM CB7 in phosphate buffer.

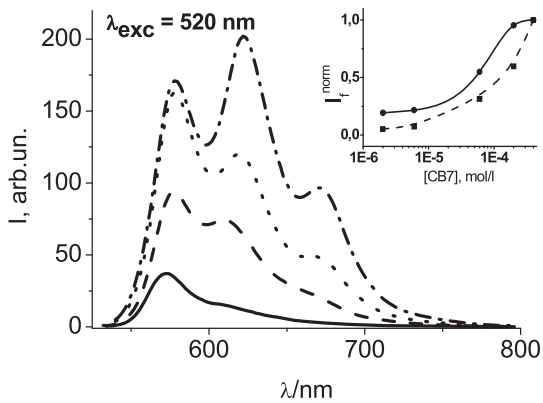

Fig. 4. Fluorescence spectra of **3** (1.5 μM) in the presence of CB7 (solid – 6 μM, dash – 60 μM, dot – 0.2 mM, dash dot – 0.5 mM) in phosphate buffer. Inset: yield of fluorescence (solid) at 578 nm of monomeric inclusion complex **3**@CB7 and (dash) at 622 nm of dimeric inclusion complex (**3**@CB7)$_2$.

vibronic transition also takes place at 650 and 700 nm for the dimeric inclusion complex of **1** and at 660 nm for that of **2**.

It should be noted that a delayed fluorescence was not observed for a dimeric inclusion complex of the thiacarbocyanine dye without alkyl *meso* substituent. We therefore suggest that alkyl substituents are a prerequisite for any delayed fluorescence of dimeric inclusion complexes. Besides the monomeric inclusion complexes also do not exhibit a delayed fluorescence.

Measurements of the fluorescence spectra of **1**–**3** in the presence of CB7 were made both under argon and in air-saturated solution. The yield of delayed fluorescence was found to decrease in air saturated solution by 8–10%. This indicates that the fluorescence comprises of both prompt and delayed fluorescence where the former contributes an essential portion of the total emission. The later almost fully disappeared under air due to quenching of the triplet state of dimeric inclusion complexes by oxygen. Fig. 5 shows the effect of oxygen on the delayed fluorescence of dimeric inclusion complexes where upon air-saturation the intensity of the peak at 606 nm for (**1**@CB7)$_2$, 622 nm for (**2**@CB7)$_2$ and 628 nm for (**3**@CB7)$_2$ is decreased 30, 25 and 20 fold respectively. The excitation spectra of the delayed fluorescence of the dimeric inclusion complexes were measured under argon in the "phosphorescence" mode (Fig. 5). Under these conditions the maxima of the excitation spectra are close to those of the absorption spectra.

An additional argument in favor of the assignment of bands to delayed fluorescence of dimeric inclusion complexes follows from temperature measurements. Fig. 6 shows the dependence of the delayed fluorescence intensity for (**3**@CB7)$_2$ upon temperature. The plot looks like a bell shape curve. The increasing of

Table 2
Maxima of delayed fluorescence (λ_{df}) and rate constants of decay of delayed fluorescence (k_{df}) for dimeric inclusion complexes in argon- and air-saturated phosphate buffer solution.

Complex	λ_{df} (nm)	k_{df} (10^3 s^{-1})	
		Under argon	Under air
(**1**@CB7$_2$)	606	2.5	14
(**2**@CB7)$_2$	622	–[a]	10
(**3**@CB7)$_2$	628, 674	0.44	4.1

[a] Not measured.

temperature in the range 5–15 °C results in the enhancement of delayed fluorescence intensity following by its decrease in the range 20–32 °C. Such a behavior of the fluorescence yield is caused by two competitive processes which are dimerization of the monomeric complexes and the population of the excited singlet state of the dimeric inclusion complexes. We suggest that at higher temperature the dissociation of (**3**@CB7)$_2$ prevails over thermally activated population of the excited singlet state (S^*) of the dimeric inclusion complexes and the concentration of S^* decreases that results in a diminishing of the fluorescence intensity. At lower temperatures population of the S^* level of the dimeric inclusion complexes decreases due to a decreasing of the rate of intersystem crossing ($T \rightarrow S^*$). In this case the concentration of S^* decreases, again leading to a decreasing of the fluorescence intensity.

Decay kinetics of the delayed fluorescence of ((**1**–**3**)@CB7)$_2$ were measured both in argon-saturated and air-saturated aqueous solution. As an example the kinetics of delayed fluorescence of (**3**@CB7)$_2$ is shown in the inset of Fig 5. The values of the rate constant of delayed fluorescence decay of the three dimeric inclusion complexes are compiled in Table 2. In argon-saturated solution the lifetime of a delayed fluorescence is 0.07, 0.1 and 0.25 ms for dimeric inclusion complexes of **1**, **2** and **3**, respectively. In air saturated solution the rate constants were found to be significantly higher than those in the absence of oxygen. This is due to quenching of the triplet state by dissolved oxygen. The observed quenching appears to be less efficient than that for many organic compounds in solvents of different polarity, where the rate of quenching is usually close to the diffusion controlled limit [42]. The reason for this low efficiency of quenching by oxygen of delayed fluorescence of ((**1**–**3**)@CB7)$_2$ is ascribed to a specific structural arrangement of the inclusion complexes, where the encounters between oxygen and **1**–**3** are expected to be hindered. Note that the solubility of air in water is 5–10 times lower than in organic solvents. Therefore, the amount of oxygen under our conditions is correspondingly lower which makes quenching less efficient.

It is noteworthy that delayed fluorescence was observed for the three alkyl *meso*-thiacarbocyanine dimeric inclusion complexes only in the presence of Na^+ and K^+ as the components of phosphate

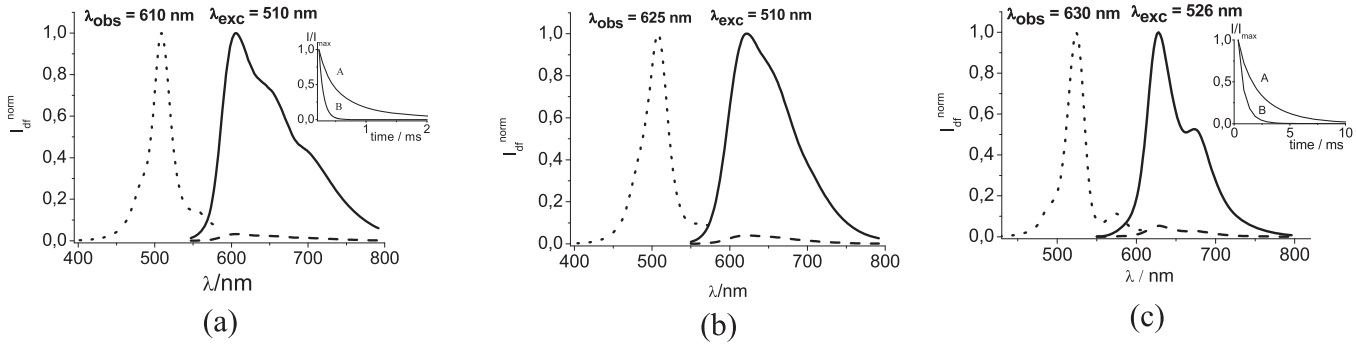

Fig. 5. Spectra of delayed fluorescence under argon (solid) and in air saturated (dash) solution and excitation spectra under argon (dot) of **1** (a), **2** (b), and **3** (c), (1.5 μM) in phosphate buffer in the presence of CB7 (1 mM). Inset: decay kinetics of delayed fluorescence of dimeric inclusion complex (**1**,**3**@CB7)$_2$ under argon (A) and air-saturation (B).

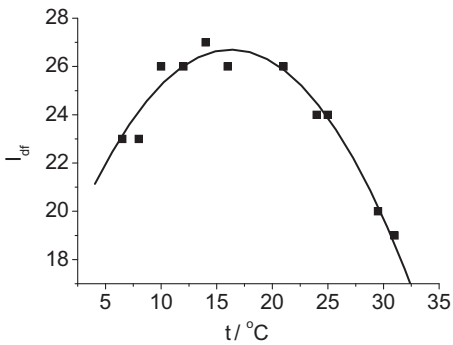

Fig. 6. Temperature dependence of the delayed fluorescence of **3** (1.5 μM) in air-saturated phosphate buffer in the presence of CB7 (0.6 mM).

buffer or in the presence of ammonium as well as on addition of Li^+ and Cs^+ to aqueous solution of ammonium hydroxide. The intensity of delayed fluorescence of dimeric inclusion complexes was found to be dependent on the size of monocations and it increases twice on passing from Li^+ to Cs^+ in the row Li^+, Na^+, K^+ and Cs^+. In contrast to monovalent metal ions, the addition of doubly (Mg^{2+}) and triply (Tb^{3+}) charged cations results in a decrease of delayed fluorescence due to replacing of the positively charged dye by metal ions. Metal ions play a double role: (i) they stimulate the dimerization process of cyanine dyes [43]; (ii) the binding of positive metal ions at the carbonyl oxygen of CB7 results in the formation of a specific kind of a plug [44] which closes the cucurbit[7]uril cavity and prevents or hinders oxygen to penetrate into the cavity [45,46].

3.3. Quantum-chemical calculations

An application in this paper of semi-empirical PM3 was dictated by the necessity to calculate the series: CB7, monomer Cy^+A^-, dimer $(Cy^+A^-)_2$, monomeric inclusion complex Cy^+A^-@CB7 and dimeric inclusion complex $(Cy^+A^-@CB7)_2$, in the frame of the consistent quantum-chemical approach. Big size of dimeric inclusion complexes, in particular, the total number of atoms in $(\mathbf{3}^+TsO^-@CB7)_2$ is 392, precludes their calculating by a more sophisticated quantum-chemical method. Here we compare energetic and structural trends for the free monomers of **1**–**3** and monomeric and dimeric inclusion complexes with CB7. Data for **2** is available in Supporting information.

Carrying out the calculations we were guided by the following considerations. (i) A relative size of the Cy and CB7 cavity implies that only one dye molecule would be inserted. Therefore, one can expect that two 'half's' of the dimers $(Cy^+A^-@CB7)_2$ are bound by π-stacking and each half being shifted relatively to each other by some angle, whereas each monomer can be situated in the cavity of its 'own' CB7. (ii) Since the dye monomer is a cation, an addition of the counter-ion is required to minimize a mutual repulsion of the chromophores in the dimers. Hence, ion pairs $\mathbf{1}^+Cl^-$, $\mathbf{2}^+Cl^-$, and $\mathbf{3}^+TsO^-$ were chosen as dye dimer components.

The questions to be answered by quantum-chemical calculations are as follows: (i) Is the semi-empirical method PM3 with the standard parameterization capable to predict a formation of the inclusion complexes of CB7 with both positive charged $\mathbf{1}^+$–$\mathbf{3}^+$ as well as with ion-pairs $\mathbf{1}^+$ Cl^-, $\mathbf{2}^+Cl^-$, and $\mathbf{3}^+TsO^-$? (ii) What geometries of the dimeric complexes $(\mathbf{1}^+Cl^-@CB7)_2$ and $(\mathbf{3}^+TsO^-@CB7)_2$ would be formed? The results of PM3 calculations of complex formation energies of **1** and **3** are compiled in Table 3. Calculated structures are shown in Figs. 7–9 for **1** and **3**.

Optimized structures of both $\mathbf{1}^+$ and $\mathbf{3}^+$ exhibit C_s symmetry. Their planes of symmetry are normal with reference to the plane of chromophores with out-of-plane ethyl groups. The positive charge in chromophores is uniformly distributed over the entire horizontal axis. Direction of a vector of dipole moment is shown by arrow. It follows from Table 3 that the formation energies of the ion pairs for $\mathbf{1}^+$ and $\mathbf{3}^+$ are 94.9 and 90 kcal mol^{-1}, respectively. Hence, the chloride anion is bound with $\mathbf{1}^+$ more strongly than the tosilate anion with $\mathbf{3}^+$ because the compact Cl^- anion (ion radius 1.81 Å) has a larger charge density than TsO^- in which a negative charge is uniformly distributed over three oxygen atoms of the sulfo group. An insertion of the positively charged $\mathbf{1}^+$ and $\mathbf{3}^+$ into the CB7 cavity to form monomer inclusion complex Cy^+@CB7 is accomplished by a lowering of the total energy by 9.3 and 21.6 kcal mol^{-1}, respectively. Consequently, owing to two chlorine substituents 3^+ reveals a more complex formation capability with CB7 than 1^+. Our calculation showed that the complex formation energies of one charged Cy^+ with CB7 are higher than those of CB7 with neutral species Cy^+A^-. This data confirms the well known facts according to which cucurbit[n]uryls are bound stronger to the positive charged ions than to neutral species. Nevertheless, the formation of the neutral complexes Cy^+A^-@CB7 is stayed on thermodynamically favourable ($\Delta E_c = -3.5$ and -15 kcal mol^{-1} for 1^+Cl^-@CB7 and 3^+TsO^-@CB7, respectively). Cl^- as counter-ion demonstrates a higher destabilized effect than TsO^- anion.

From Fig. 7b, it is seen that $\mathbf{3}^+$@CB7 is a real inclusion complex because one chlorophenyl moiety of the dye and partially the thiazole group are positioned into the cavity.

Cyanine dyes are known to be capable of forming dimeric species [25] and our calculations confirm this observation. The structure of dye dimers is shown in Fig. 8.

Vectors of dipole moment of both choromophores in the dye dimers are oriented anti-parallel to each other and the components are bound by π-stacking interaction [47]. The dimerization energy of $\mathbf{3}^+TsO^-$ was calculated to be 9.7 kcal mol^{-1} (Table 3) whereas dimerization of its counterpart $\mathbf{1}^+Cl^-$ proceeds with elimination of less energy (6.3 kcal mol^{-1}). The data on the lower capability of **1** relatively to **3** to dimerize and insert into the CB7 cavity is in a good agreement with the spectral behaviour of these dyes. Indeed, UV spectra of the latter demonstrate the presence of the higher concentration of dimers and complexes with CB7 than those of **1**.

The structures of the dimer complexes $(\mathbf{1}^+Cl^-@CB7)_2$ and $(\mathbf{3}^+TsO^-@CB7)_2$ optimized by PM3 are shown in Fig. 9 and presented as balls using Chemcraft version 1.7. rendering options.

The total formation energy (-22.3 kcal mol^{-1}) of $(\mathbf{3}^+TsO^-@CB7)_2$ is high enough to hold the components close to each other. Additional stabilization of $(\mathbf{3}^+TsO^-)_2$ due to its insertion into CB7 cavities is 12.6 kcal mol^{-1}.

The complex has a C_i symmetry, , it is central symmetric. The structure of the complex demonstrates that, indeed, only one dye molecule is present in the cavity. The $\mathbf{3}^+$, being inserted into the cavity of CB7, retains a practically planar configuration of the chromophore because one half of the each dye molecule turned around the central allyl bond merely by 2.2°. The dimer

Table 3
Complex formation energy ΔE_c (in units of kcal mol^{-1}) calculated by PM3 for ion-pairs $\mathbf{1}^+Cl^-$,$\mathbf{3}^+TsO^-$, $(\mathbf{1}^+Cl^-)_2$, $(\mathbf{3}^+TsO^-)_2$ and monomeric inclusion complexes $\mathbf{1}^+$@CB7, $\mathbf{3}^+$@CB7 and dimeric inclusion complexes $(\mathbf{1}^+Cl^-@CB7)_2$, $(\mathbf{3}^+TsO^-@CB7)_2$.

Dye and complexes with CB7	ΔE_c	Dye and complexes with CB7	ΔE_c
$\mathbf{1}^+Cl^-$	−94.9[a]	$\mathbf{3}^+TsO^-$	−90.0[a]
$(\mathbf{1}^+Cl^-)_2$	−6.3[b]	$(\mathbf{3}^+TsO^-)_2$	−9.7[b]
$\mathbf{1}^+$@CB7	−9.3	$\mathbf{3}^+$@CB7	−21.6
$\mathbf{1}^+Cl^-$@CB7	−3.5	$\mathbf{3}^+TsO^-$@CB7	−15.0
$(\mathbf{1}^+Cl^-@CB7)_2$	−14.5	$(\mathbf{3}^+TsO^-@CB7)_2$	−22.3

Structures of $\mathbf{3}^+$ and its complex $\mathbf{3}^+$@CB7 are shown in Fig. 7.
[a] Energy of formation of ion-pair Cy^+A^-.
[b] Dimerization energy.

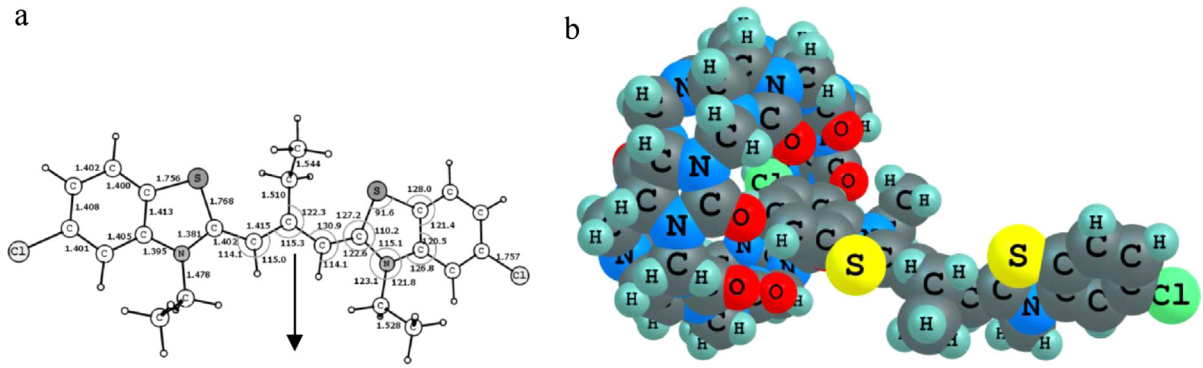

Fig. 7. Structures of $\mathbf{3}^+$(a) and $\mathbf{3}^+$@CB7 (b) calculated by PM3. Arrow shows the direction of the dipole moment. C-atoms are shown as grey balls, O-atoms – red those, Cl-atoms – light green those, S-atoms – yellow those, N-atoms – dark blue those, H-atoms – blue those. (For interpretation of the references to color in this figure legend, the reader is referred to the web version of this article.)

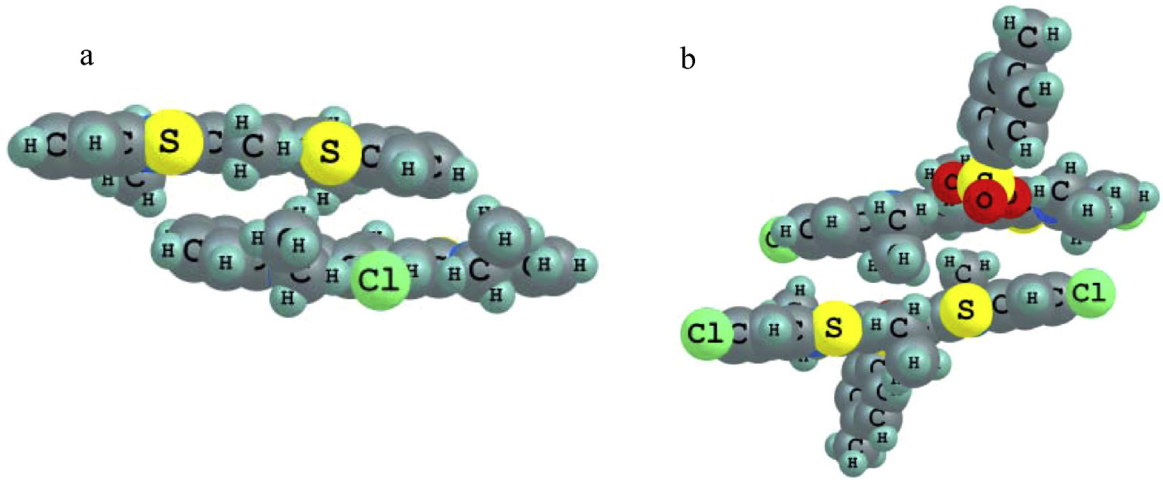

Fig. 8. Structure of dimers $(\mathbf{1}^+Cl)_2$ (a) and $(\mathbf{3}^+TsO)_2$ (b) optimized by PM3 and presented as balls using rendering options in Chemcraft with version 1.7. C-atoms are shown as grey balls, O-atoms – red those, Cl-atoms – light green those, S-atoms – yellow those, N-atoms – dark blue those, H-atoms – blue those. (For interpretation of the references to color in this figure legend, the reader is referred to the web version of this article.)

components being positioned parallel to each other are linked together by both π-stacking and partial insertion of the chromophoric group into the CB7 cavity. It can be seen from Fig. 9 that terminal chlorine atoms of each dye molecule are completely located into the cavities of its "own" CB7, as it was predicted from geometrical considerations. Note that the mean distance between the planes of choromophores is calculated to be 4.3 Å and the angle shift α between choromophoric planes in the dimer is 52°.

For a dimer, the angle α is defined as that between two terminal C atoms of the upper and lower chromophores and the central C allyl atom of the lower one (Fig. 9a); by definition $\alpha = 90°$ for face-to-face alignment of the structure. According to exciton theory [48], the absorption bands of dimers with $\alpha > 50°$ should be blue-shifted compared to those of the monomers. It is seen from Fig. 1 that the blue-shift of the absorption band in a dimer is 37 nm. The transition energies (as expressed by λ in nm) were calculated for $\mathbf{3}^+$ and its dimeric inclusion complex $(\mathbf{3}^+TsO^-@CB7)_2$ using the semi-empirical ZINDO/S method (HyperChem package). This semi-empirical method was shown to predict correctly spectral band shifts caused by the dye aggregation [47]. The blue-shift of the absorption maximum was calculated to be $\Delta\lambda = 18$ nm (462 and 444 nm, for $\mathbf{3}^+$ and $(\mathbf{3}^+TsO^-@CB[7])_2$, respectively). A further increase of α up to 79° results in a further blue-shift of $\Delta\lambda = 23$ nm. Therefore, the ZINDO/S method predicts the trend of the spectral shift although the real α value can be higher than the calculated one of 52°.

The calculation shows that complex $(\mathbf{1}^+Cl^-@CB7)_2$ exists (Fig. 9a) also although as one can expect that it is less stable (ΔE_c −14 kcal mol^{-1}). The structural motif of $(\mathbf{1}^+Cl^-@CB7)_2$ resembles that of $(\mathbf{3}^+TsO^-@CB7)_2$. However, in the former, the dye molecules are not inserted into the CB7 cavity, i.e., PM3 calculation results in the formation of an outer complex between $\mathbf{1}^+\cdot Cl^-$ dimers and two CB7. The structure of $(\mathbf{1}^+Cl^-@CB7)_2$ is shown in Supporting information.

Thereby, the results of quantum-chemical calculations corroborate the formation of dimeric inclusion complexes of $\mathbf{3}^+TsO^-$ with CB7 in which both chromophores retain a plane structure. The dimers of alkyl *meso*-thiacarbocyanine dyes were shown to populate the triplet level much more efficient than the monomers [32], and consequently delayed fluorescence of dimeric inclusion complexes with CB7 is quite reasonable. A similar conclusion concerning the dimeric structure has recently been made for the complex of a monomethine cyanine (thiazole orange) in cucurbit [8]uril [35]. A propensity of cyanine dyes to dimerization has been established for certain carbocyanines [43].

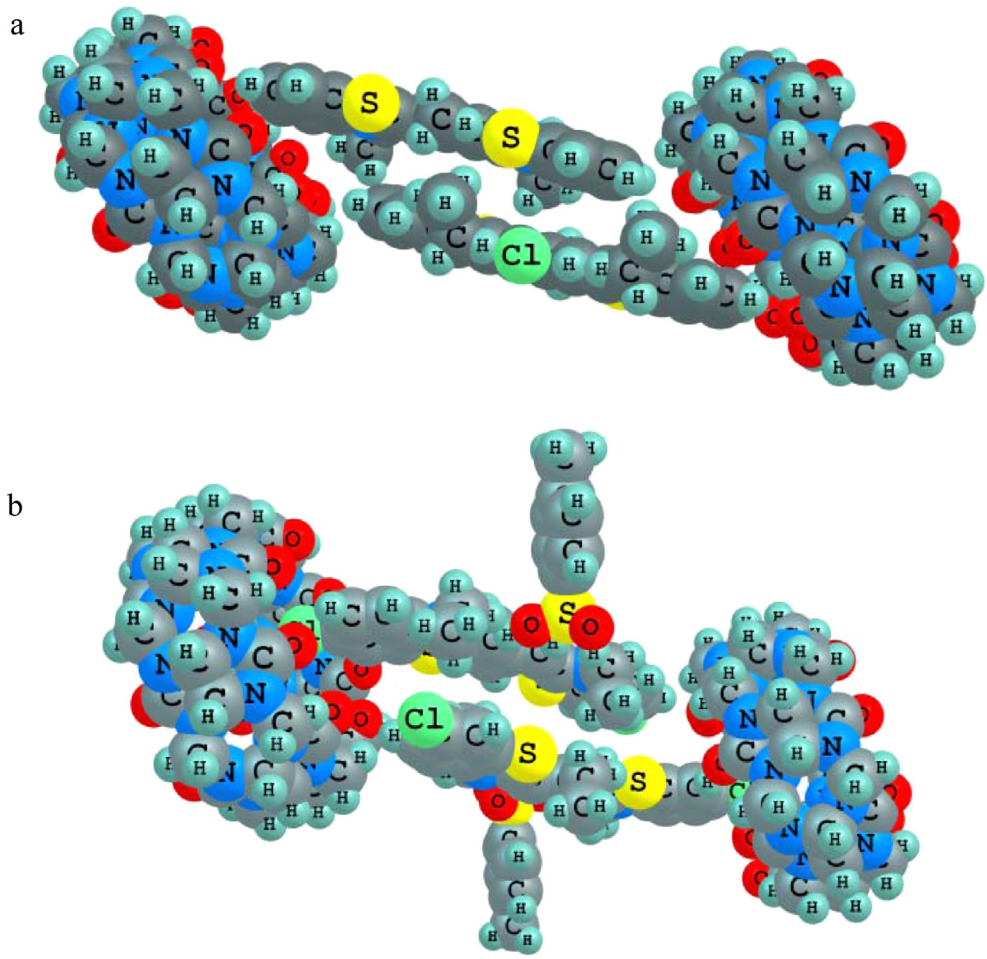

Fig. 9. Structure of the dimeric inclusion complexes ($\mathbf{1}^{+}Cl^{-}$@CB7)$_2$ (a) and ($\mathbf{3}^{+}TsO^{-}$@CB7)$_2$ (b) optimized by PM3 and presented as balls using rendering options in Chemcraft with version 1.7. C-atoms are shown as grey balls, O-atoms – red those, Cl-atoms – light green those, S-atoms – yellow those, N-atoms – dark blue those, H-atoms – blue those. (For interpretation of the references to color in this figure legend, the reader is referred to the web version of this article.)

4. Conclusions

Cationic dyes of three alkyl *meso*-thiacarbocyanines are present in aqueous solution as a mixture of monomers and dimers. The monomers show a significant increase of fluorescence yield in the presence of CB7 as a result of formation of monomeric inclusion complexes. The dimeric inclusion complexes exhibit both prompt and delayed fluorescence with much smaller intensity for the later (0.08–0.1 of the total emission). The smaller yield in air-saturated solution is due to quenching of the triplet state of dimeric complexes by oxygen. The existence of alkyl groups in the *meso*-position of thiacarbocyanines as well as the presence of monovalent metal ions or ammonium cation are prerequisites for delayed fluorescence of dimeric inclusion complexes. Quantum-chemical calculations corroborate the experimental results on the formation of dimeric inclusion complexes which are characterized by near parallel orientation of two π-stacking chromophores retaining planar configuration whereby each of them is partly inserted into the CB7 inner cavity, and, consequently, delayed fluorescence of dimeric complexes with CB7 is quite reasonable.

Acknowledgement

This work was supported by the Russian Foundation for Basic Researches (Project Nos. 15-03-01524 and 15-03-01835).

Appendix A. Supplementary data

Supplementary data associated with this article can be found, in the online version, at http://dx.doi.org/10.1016/j.jphotochem.2015.01.011.

References

[1] W.L. Mock, Cucurbituril, Top. Curr. Chem. 175 (1995) 1–24.
[2] C. Marquez, R.R. Hudgins, W.M. Nau, Mechanism of host–guest complexation by cucurbituril, J. Am. Chem. Soc. 126 (2004) 5806–5816.
[3] O.A. Gerasko, D.G. Samsonenko, V.P. Fedin, Supramolecular chemistry of cucurbiturils, Russ. Chem. Rev. 71 (2002) 840–861.
[4] Y.J. Jeon, Y.H. Ko, S. Sakamoto, K. Yamaguchi, K. Kim, Novel molecular drug carrier: encapsulation of oxaliplatin in cucurbit[7]uril and its effects on stability and reactivity of the drug, Org. Biomol. Chem. 3 (2005) 2122–2125.
[5] J.M. Lehn, Supramolecular Chemistry: Concepts and Perspectives, VCH, Weinheim, 1995.
[6] S.H. Gellman, Introduction: molecular recognition, Chem. Rev. 97 (1997) 1231–1232.
[7] S.Y. Jon, Y.H. Ko, S.H. Park, H.J. Kim, K.A. Kim, Facile, stereoselective [2+2] photoreaction mediated by cucurbit[8]uril, Chem. Commun. 19 (2001) 1938–1939.
[8] M. Pattabraman, A. Nararajan, R. Kaliappan, J.T. Mague, V. Ramamurthy, Template directed photodimerization of *trans*-1,2-bis(*n*-pyridyl)-ethylenes and stilbazoles in water, Chem. Commun. 36 (2005) 4542–4544.
[9] S.P. Gromov, A.I. Vedernikov, L.G. Kuz'mina, D.V. Kondratuk, S.K. Sazonov, M.V. Strelenko, J.A.K. Howard, Photocontrolled molecular assembler based on cucurbit[8]uril: [2+2]-autophotocycloaddition of styryl dyes in solid state and in water, Eur. J. Org. Chem. (2010) 2587–2599.
[10] A.L. Koner, W.M. Naw, Cucurbituril encapsulation of fluorescent dyes, Supramol. Chem. 19 (2007) 55–66.

[11] R.L. Halterman, J.L. Moore, K.A. Yakshe, J.A.L. Halterman, K.A. Woodson, Inclusion complexes of cationic xanthene dyes in cucurbit[7]uril, J. Inclusion Phenom. Macrocyclic Chem. 66 (2010) 231–241.
[12] W.M. Nau, J. Mohanty, Taming fluorescent dyes with cucurbituril, Int. J. Photoenergy 7 (2005) 133–141.
[13] R.N. Dsouza, U. Pischel, W.M. Nau, Fluorescent dyes and their supramolecular host/guest complexes with macrocycles in aqueous solution, Chem. Rev. 111 (2011) 7941–7980.
[14] J. Mohanty, W.M. Nau, Ultrastable rhodamine with cucurbituril, Angew. Chem. Int. Ed. Engl. 44 (2005) 3750–3754.
[15] Y.Y. Zhou, H.P. Yu, L. Zhang, G.Y. Sun, L. Wu, Q. Lu, L. Wang, Host properties of cucurbit [7]uril: fluorescence enhancement of acridine orange, J. Inclusion Phenom. Macrocyclic Chem. 61 (2008) 259–264.
[16] H.P. Yu, G.Y. Sun, L. Wu, H. Xu, L. Wang, Y.Y. Zhou, Study on the inclusion behavior of cucurbit[7]uril with methylene blue by spectrofluorometric titrations, Spectr. Anal. 29 (2009) 1041–1044.
[17] A.C. Bhasikuttan, J. Mohanty, W.M. Nau, H. Pal, Efficient fluorescence enhancement and cooperative binding of an organic dye in a supra-biomolecular host-protein assembly, Angew. Chem. Int. Ed. 46 (2007) 4120–4122.
[18] E. Arunkumar, C.C. Forbe, B.D. Smith, Improving the properties of organic dyes by molecular encapsulation, Eur. J. Org. Chem. 405 (2005) 4051–4059.
[19] N. Kh Petrov, D.A. Ivanov, D.V. Golubkov, S.P. Gromov, M.V. Alfimov, The effect of cucurbit[7]uril on photophysical properties of aqueous solution of 3,3'-diethylthiacarbocyanine iodide dye, Chem. Phys. Lett. 480 (2009) 96–99.
[20] N. Tyutyulkov, J. Fabian, A. Mehlhorn, F. Dietz, A. Tadjer, Polymethine Dyes, St. Kliment Ohridski University Press, Sofia, 1991.
[21] A. Mishra, R.K. Behera, P.K. Behera, B.K. Mishra, G.B. Behera, Cyanines during the 1990: a review, Chem. Rev. 100 (2000) 1973–2011.
[22] B.H. Carroll, G.C. Higgins, T.H. James, Introduction to photographic theory, The Silver Halide Process, Wiley, New York, 1980.
[23] D.M. Sturmer, D.W. Heseltine, Sensitizing and desensitizing dyes, in: T.H. James (Ed.), The Theory of the Photographic Processes, fourth ed., Macmillan, New York, 1977, pp. 194–234.
[24] I. Mal'tsev, D.A. Lypenko, B.I. Shapiro, M.A. Brusentseva, G.H.W. Milburn, J. Wright, A. Hendriksen, V.I. Berendyaev, B.V. Kotov, A.V. Vannikov, Electroluminescence of polymer/J-aggregate composites, Appl. Phys. Lett. 75 (1999) 1896–1898, doi:http://dx.doi.org/10.1063/1.124864.
[25] I.G. Scheblykin, L.S. Lepnev, A.G. Vitukhnovsky, M. Van der Auweraer, Electroluminescence and optical properties of poly(phenylenevinylene)/J-aggregate composites, J. Lumin. 94 (2001) 461–464, doi:http://dx.doi.org/10.1016/S0022-2313(01)00337-4.
[26] S. Bourbon, M.Y. Gao, S. Kirstein, Electroluminescence of self-assembled films of poly (*p*-phenylene vinylene) and J-aggregates, Synth. Met. 101 (1999) 152–153, doi:http://dx.doi.org/10.1016/S0379-6779(98)00513-X.
[27] F. Sasaki, S. Kobayashi, Effects of photoreaction to optical nonlinearities in pseudoisocyanine, J. Lumin. 72–74 (1997) 538–540, doi:http://dx.doi.org/10.1016/S0022-2313(96)380-8.
[28] A.S. Tatikolov, Polymethine dyes as spectral-fluorescent probes for biomacromolecules, J. Photochem. Photobiol. C 13 (2012) 55–90, doi:http://dx.doi.org/10.1016/j.jphotochemrev.2011.11.001.
[29] H. Görner, A.K. Chibisov, Photoprocesses in polymethine dyes: cyanines and spiropyrane-derivative merocyanines, in: W. Horspool, F. Lenci (Eds.), CRC Handbook of Organic Photochemistry and Photobiology, second ed., CRC PRESS, Boca Raton–London–New York–Washington, 2004, pp. 36-1–36-21.
[30] L.S. Atabekyan, N.A. Kulemin, V.G. Avakyan, A.K. Chibisov, Molecular photonics of inclusion complexes of cucurbit[7]uril with 3,3′-diethylthiazolinocarbocyanine iodide, Russ Chem. Bull. Int. Ed. 62 (2013) 966–975.
[31] G.V. Zakharova, D.A. Zhizhimov, V.G. Avakyan, S.K. Sazonov, S.P. Gromov, A.K. Chibisov, Specificity of photonics of 3,3′-diethyl-5,5′-dichloro-9-ethylthiacarbocyanine dimers in the presence of cucurbit[7]uril, High Energy Chem. 48 (2014) 76–80.
[32] A.K. Chibisov, Photonics of dimers of cyanine dyes, High Energy Chem. 41 (2007) 200–209.
[33] A.H. Herz, Dye–dye interactions of cyanines in solution and at AgBr surfaces, Photogr. Sci. Eng. 18 (1974) 323–335.
[34] A.K. Chibisov, G.V. Zakharova, H. Görner, Photoprocesses of thiamonomethinecyanine monomers and dimmers, Phys. Chem. Chem. Phys. 3 (2001) 44–49, doi:http://dx.doi.org/10.1039/b005683i.
[35] J. Mohanty, N. Thakur, S.D. Choudhury, N. Baroah, H. Pal, A.C. Bhasikuttan, Recognition-mediated light-up of thiazole orange with cucurbit[8]uril: exchange and release by chemical stimuli, J. Phys. Chem. B 116 (2012) 130–135.
[36] A.K. Chibisov, T.D. Slavnova, G.V. Zakharova, H. Görner, Primary processes in the photosensitized redox reaction of dimers of thiacarbocyanine dyes, High Energy Chem. 41 (2007) 344–349, doi:http://dx.doi.org/10.1134/S0018143907050074.
[37] S. Navaratnam, B.J. Parsons, Kinetic and spectral properties of rhodamine 6G free radicals: a pulse radiolysis study, J. Photochem. Photobiol. A 153 (2002) 153–162, doi:http://dx.doi.org/10.1016/S1010-6030(02)265-4.
[38] T.D. Slavnova, A.K. Chibisov, H. Görner, Photoprocesses of thiacarbocyanine monomers dimers, and aggregates bound to polyanions, J. Phys. Chem. A 106 (2002) 10985–10990.
[39] V. Khimenko, A.K. Chibisov, H. Görner, Effects of alkyl substituents in the polymethine chain on the photoprocesses in thiacarbocyanine dyes, J. Phys. Chem. A 101 (1997) 7304–7310.
[40] K.G. Vladimirova, A.Y. Freidzon, A.A. Bagatur'yants, G.V. Zakharova, A.K. Chibisov, M.V. Alfimov, Modeling the structure, absorption spectra, and *cis–trans* isomerization of thiacarbocyanine dyes, High Energy Chem 42 (2008) 275–282.
[41] P. Gans, A. Sabatini, A. Vacca, Investigation of equilibria in solution. Determination of equilibrium constants with the HYPERQUAD suite of programs, Talanta 43 (1996) 1739–1753.
[42] M.Z. Hoffman, F. Bolletta, L. Moggi, G.L. Hug, Rate constants for the quenching of excited-states of metal-complexes in fluid solution, J. Phys. Chem. Ref. Data 18 (1989) 219–544.
[43] T.D. Slavnova, A.K. Chibisov, H. Görner, Kinetics of salt-induced J-aggregation of cyanine dyes, J. Phys. Chem. C 109 (2005) 4758–4765.
[44] K.B. Tormyshov, F. Müller-Plathe, Ion binding to cucurbit[6]uril: structure and dynamics, J. Phys. Chem. B 110 (2006) 14463–14468.
[45] S.D. Choudhury, J. Mohanty, H. Pal, A.C. Bhasikuttan, Cooperative metal ion binding to a cucurbit[7]uril-thioflavin T complex: demonstration of a stimulus-responsive fluorescent supramolecular capsule, J. Am. Chem. Soc. 132 (2010) 1395–1401.
[46] A.C. Bhasikuttan, S.D. Choudhury, H. Pal, J. Mohanty, Supramolecular assemblies of thioflavin T with cucurbiturils: prospects of cooperative and competitive metal ion binding, Isr. J. Chem. 51 (2011) 634–645.
[47] V.G. Avakyan, B.I. Shapiro, M.V. Alfimov, Dimers tetramers, and octamers of mono- and trimethyne thiacarbocyanine dyes. Structure, formation energy, and absorbtion band shifts, Dyes Pigm. 109 (2014) 21–33.
[48] P.O.J. Scherer, Molecular aggregate spectra, in: T. Kobayashi (Ed.), J-aggregates, World Scientific, Singapore–New Jersey–London–Hong Kong, 1996, pp. 95–110.